No evident charge ordering in $La_{1/2}Sr_{3/2}MnO_4$

2002 J. Phys.: Condens. Matter 14 4659

(http://iopscience.iop.org/0953-8984/14/18/303)

INSTITUTE OF PHYSICS PUBLISHING JOURNAL OF PHYSICS: CONDENSED MATTER

J. Phys.: Condens. Matter **14** (2002) 4659–4667 PII: S0953-8984(02)34404-7

No evident charge ordering in $La_{1/2}Sr_{3/2}MnO_4$

J Wang, Weiyi Zhang and D Y Xing

National Laboratory of Solid State Microstructures and Department of Physics, Nanjing University, Nanjing 210093, People's Republic of China

Received 28 February 2002
Published 26 April 2002
Online at stacks.iop.org/JPhysCM/14/4659

Abstract

Using the unrestricted Hartree–Fock approximation to deal with the correlation effect of the multiband Hubbard model and the real-space recursion method to calculate the density of states, we have investigated several assumed spin- and orbital-ordered states in the layered perovskite $La_{1/2}Sr_{3/2}MnO_4$ in addition to the so-called charge-exchange-type antiferromagnetic (CE-AFM) state observed experimentally. It is found that the Jahn–Teller lattice distortion and anisotropic double-exchange interaction of e_g electrons are responsible for the CE-AFM state with $d_{3x^2-r^2}/d_{3y^2-r^2}$ orbital ordering. Our study shows that there is no evident charge modulation in real space, which is consistent with recent band-structure calculation (Mahadevan P, Terakura K and Sarma D D 2001 *Phys. Rev. Lett.* **87** 066404). We attribute this to the strong double-exchange interaction inside the quasi-one-dimensional ferromagnetic zigzag chain that is the basic building block of the CE-AFM state.

1. Introduction

Recently, manganites of perovskite structure $R_{1-x}A_xMnO_3$ (R: rare-earth elements, A: alkaline-earth elements) have attracted a great deal of attention due to the rediscovery of colossal magnetoresistance (CMR) [1] as well as the exotic phenomena arising from strong coupling among spin, charge, and orbital degrees of freedom [2]. A prototype compound is half-doped $Nd_{1/2}Sr_{1/2}MnO_3$ [3], where the charge-exchange-type antiferromagnetic (CE-AFM) state with charge ordering (CO) and orbital ordering (OO) was proposed by Goodenough [4] as a candidate state at low temperature. Every Mn^{3+} ion is surrounded by Mn^{4+} ions and vice versa, like a checkerboard, as shown in figure 1. The whole pattern is composed of ferromagnetic (FM) quasi-one-dimensional zigzag chains that are coupled antiferromagnetically with each other. In the MnO_2 plane (*ab*-plane), one e_g electron of a Mn^{3+} site occupies either the $d_{3x^2-r^2}$ or the $d_{3y^2-r^2}$ orbital. This anomalous magnetic structure as well as the corresponding Jahn–Teller lattice distortion (JTD) of Mn^{3+} sites have been confirmed by different experiments such as x-ray and neutron diffraction measurements [5]. In addition to the three-dimensional perovskites, the same CE-AFM state has also been observed experimentally in

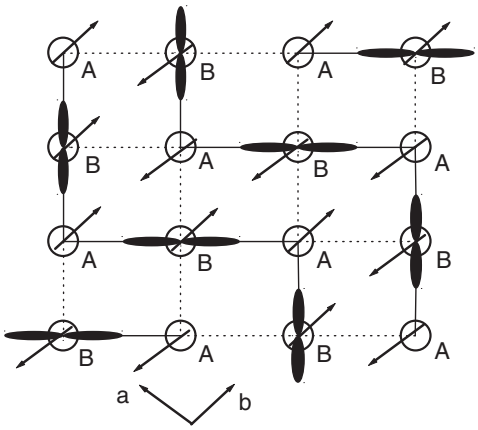

Figure 1. Spin, charge, and OO for the CE-type AFM CO state in the *ab*-plane. Symbols A and B stand respectively for Mn^{4+} sites and Mn^{3+} sites.

layered perovskite $La_{1/2}Sr_{3/2}MnO_4$, which has two-dimensional characterization. The elastic neutron scattering measurements by Sternlieb *et al* [6] demonstrate that $La_{1/2}Sr_{3/2}MnO_4$ has charge and magnetic ordering transitions at $T_{CO} \sim 217$ K and $T_N \sim 110$ K, respectively. Murakami *et al* [7], using the anisotropy of the x-ray scattering tensor, have shown the alternating pattern of Mn^{3+}/Mn^{4+} in real space.

Theoretically, the microscopic mechanism behind the CE-AFM state has been seen as an intriguing subject since the spin, charge, and OOs are closely related to the transport properties of compounds. Solovyev and Terakura [8], solving analytically a simple quasi-1D model, argued that the trigger for CO lies in the unique insulating features of the quasi-1D FM zigzag chain, and the $d_{3x^2-r^2}/d_{3y^2-r^2}$ OO is entirely determined by the kinetic effects. Mizokawa and Fujimori [9] emphasized that JTD plays an important role in stabilizing the CE-AFM state since, in their calculation, the FM state would be more favourable than that without JTD; this was demonstrated by other first-principles band-structure calculations, too [10, 11]. Strong electron–electron interactions, such as on-site Coulomb and nearest-neighbour Coulomb interaction [12], were also proposed to interpret this interesting spin-, charge-, and orbital-ordered state. However, which are the crucial factors leading to the CE-AFM state is still an open issue.

A recent band calculation on $La_{1/2}Sr_{3/2}MnO_4$ by Mahadevan *et al* [11] suggests that the CE-AFM state has no substantial CO in real space but has an evident OO. They calculated the Mn 4p partial density of states and argued that the OO, causing two different Mn-ion environments, is sufficient for interpreting the experimental phenomenon, i.e., the observed anisotropy of the x-ray scattering tensor [7]. Thus, the reason that OO and *charge ordering* transitions occur over the same temperature range experimentally is that there is no real CO in $La_{1/2}Sr_{3/2}MnO_4$; the observed anisotropic scattering tensor is just a manifestation of the same lattice distortion. In fact, Solovyev and Terakura [8] acknowledged that charge inhomogeneity tends to destroy the intrachain ferromagnetism in the CE-AFM state, i.e., CO is unfavourable to FM. Jung *et al* [13] used the scenario of states with bonding and antibonding between $d_{3x^2-r^2}$ ($d_{3y^2-r^2}$) of Mn^{3+} and $d_{x^2-y^2}$ of Mn^{4+} to explain well the temperature dependence of the optical conductivity spectrum of $La_{1/2}Sr_{3/2}MnO_4$. It seems that such a strong effect of covalent bonding between Mn^{3+} and Mn^{4+} ions should not make an e_g electron localize on a particular orbital unless one energy level is much lower than the other—similar to the case for the *polar molecule*.

The purpose of this paper is now clear. One objective is to study what factors will be important in stabilizing the observed CE-AFM state in $La_{1/2}\,Sr_{3/2}MnO_4$ and another is to see whether there is any charge modulation in real space. Thus, we employ unrestricted Hartree–Fock (HF) approximation in the multiband d–p Hubbard model to treat several assumed magnetically and orbitally ordered states, besides the CE-AFM state, on the same footing. By comparing these ordered states, we show that the JTD and the anisotropy of double exchange of e_g electrons lead to the CE-AFM state. Our calculations demonstrate that there is indeed no evident charge modulation in $La_{1/2}Sr_{3/2}MnO_4$ in comparison with the antiferromagnetic and charge-ordered ground states of other compounds; we argue that it is difficult for an e_g electron to localize strongly on a site due to the strong double-exchange interaction inside a FM zigzag chain.

The rest of the paper is organized in the following way. In section 2, we introduce the multiband d–p lattice model and the unrestricted HF approximation; then the real-space recursion method is also briefly outlined. In section 3, we present the numerical results on several calculated ordered states and a discussion on the origin of the CE-AFM state. Conclusions are drawn in section 4.

2. Theoretical model and formulation

To describe the perovskite compound in the presence of lattice distortion, we have extended the widely adopted multiband d–p model to include the generalized Jahn–Teller effect on the fivefold d orbitals. The Hamiltonian can be written in terms of the electronic part $\mathcal{H}_e$ and the electron–phonon coupling $\mathcal{H}_{ep}$: $\mathcal{H} = \mathcal{H}_e + \mathcal{H}_{ep}$, where $\mathcal{H}_e$ includes the full degeneracies of the transition-metal 3d orbitals and oxygen 2p orbitals as well as the on-site Coulomb and exchange interaction; it can be expressed as [14]

$$\begin{aligned}\mathcal{H}_e = &\sum_{im\sigma} \varepsilon^0_{dm} d^\dagger_{im\sigma} d_{im\sigma} + \sum_{jn\sigma} \varepsilon_p p^\dagger_{jn\sigma} p_{jn\sigma} \\ &+ \sum_{ijmn\sigma} (t^{mn}_{ij} d^\dagger_{im\sigma} p_{jn\sigma} + \text{H.c.}) + \sum_{ijnn'\sigma} (t^{nn'}_{ij} p^\dagger_{in\sigma} p_{jn'\sigma} + \text{H.c.}) \\ &+ \sum_{im} u d^\dagger_{im\uparrow} d_{im\uparrow} d^\dagger_{im\downarrow} d_{im\downarrow} + \tfrac{1}{2} \sum_{im\neq m'\sigma\sigma'} \tilde{u} d^\dagger_{im\sigma} d_{im\sigma} d^\dagger_{im'\sigma'} d_{im'\sigma'} \\ &- j \sum_{im\sigma\sigma'} d^\dagger_{im\sigma} \sigma d_{im\sigma'} S^d_{im}. \end{aligned} \tag{1}$$

In equation (1), $d_{im\sigma}$ ($d^\dagger_{im\sigma}$) and $p_{jn\sigma}$ ($p^\dagger_{jn\sigma}$) denote the annihilation (creation) operators of an electron on Mn d at site i and O p at site j, respectively, and ε^0_{dm} and ε_p are their corresponding on-site energies; m and n represent the orbital index and σ denotes the spin. The crystal-field splitting is included in ε^0_{dm}, i.e., $\varepsilon^0_d(t_{2g}) = \varepsilon^0_d - 4Dq$, $\varepsilon^0_d(e_g) = \varepsilon^0_d + 6Dq$. ε^0_d is the bare on-site energy of the d orbital. t^{mn}_{ij} and $t^{nn'}_{ij}$ are the nearest-neighbour hopping integrals for p–d and p–p orbitals; they are expressed in terms of Slater–Koster parameters (pdσ), (pdπ), (ppσ), and (ppπ). S^d_{im} is the total spin operator of the Mn ion extracting the one in orbital m; $\tilde{u} = u - 5j/2$. The parameter u is related to the multiplet-averaged d–d Coulomb interaction U via $u = U + (20/9)j$. After linearizing the above Hamiltonian using the unrestricted HF approximation, $\mathcal{H}_e$ becomes

$$\begin{aligned}\mathcal{H}_e = &\sum_{im\sigma} \left[\varepsilon^0_{dm} + u n^d_{im\bar{\sigma}} - \frac{j}{2}\sigma(\mu^d_t - \mu^d_m) + \tilde{u}(n^d_t - n^d_m) \right] d^\dagger_{im\sigma} d_{im\sigma} \\ &+ \sum_{jn\sigma} \varepsilon_p p^\dagger_{jn\sigma} p_{jn\sigma} + \sum_{ijmn\sigma} (t^{mn}_{ij} d^\dagger_{im\sigma} p_{jn\sigma} + \text{H.c.}) \end{aligned}$$

$$+ \sum_{ijnn'\sigma} (t_{ij}^{nn'} p_{in\sigma}^{\dagger} p_{jn'\sigma} + \text{H.c.}). \tag{2}$$

Here $n_{m\sigma}^d = \langle d_{m\sigma}^{\dagger} d_{m\sigma} \rangle$, $\mu_m^d = n_{m\uparrow}^d - n_{m\downarrow}^d$, and n_t^d and μ_t^d are the total electron numbers and magnetization of the Mn d orbitals. We have chosen the z-axis as the spin quantization axis.

Before we derive the $\mathcal{H}_{ep}$ part, let us assume that oxygen ions move only along the direction of the Mn–O–Mn bond so that rotation of MnO_6 octahedra and the buckling of the Mn–O–Mn bond are not considered, for simplicity. The dimensionless lattice distortion is defined as $Q_a(i) = (u_a(i + \frac{1}{2}a) - u_a(i - \frac{1}{2}a))/a$ which describes the local expansion of oxygens along the a-axis around the ith Mn ion; $u_a(i \pm \frac{1}{2}a)$ represents the displacement of oxygen ions with $a = x$, y, and z. On expanding the local static Coulomb potential $V(r) = \sum_j \frac{Ze}{|r-r_j|}$ around Mn ions to fourth order, the deviation from the equilibrium positions gives rise to Jahn–Teller coupling between the d orbitals and octahedra distortion $Q_a(i)$. Note that r_j represents the neighbouring oxygen ions around a Mn ion and Ze is the effective charge of O ions. We obtain

$$\begin{aligned}\mathcal{H}_{ep} = \sum_{i\sigma}\Bigg(-g_1 Q_1(i) \sum_m d_i^{\dagger} d_i - g_2\Bigg[& Q_3(i) d_{xy\sigma}^{\dagger} d_{xy\sigma} \\ & + \left(\frac{\sqrt{3}}{2} Q_2(i) - \frac{1}{2} Q_3(i)\right) d_{yz\sigma}^{\dagger} d_{yz\sigma} + \left(-\frac{\sqrt{3}}{2} Q_2(i) - \frac{1}{2} Q_3(i)\right) d_{zx\sigma}^{\dagger} d_{zx\sigma} \\ & + (d_{x^2-y^2\sigma}, d_{3z^2-r^2\sigma}) \begin{pmatrix} Q_3(i) & Q_2(i) \\ Q_2(i) & -Q_3(i) \end{pmatrix} \begin{pmatrix} d_{x^2-y^2\sigma} \\ d_{3z^2-r^2\sigma} \end{pmatrix}\Bigg]\Bigg).\end{aligned} \tag{3}$$

Here Q_1, Q_2, and Q_3 are the three Jahn–Teller modes and they are related to the displacement of the oxygen atoms along the a-, b-, and c-axes via $Q_1 = (Q_a + Q_b + Q_c)/\sqrt{3}$, $Q_2 = (Q_b - Q_a)/\sqrt{2}$, and $Q_3 = (Q_a + Q_b - 2Q_c)/\sqrt{6}$. While Q_1 is the usual breathing mode and involves local volume contraction or expansion, Q_2 and Q_3 are the usual vibration modes and conserve the local volume [15]. Their corresponding coupling constants are $g_1 = \frac{4\sqrt{3}2Ze^2}{a_0}$ and $g_2 \simeq 0.6892(10Dq\ g_1)^{1/2}$.

For the effective single-particle Hamiltonian discussed above, the density of states can be easily calculated using the real-space recursion method [16] and the Green function is expressed as

$$G_{m\sigma}^0(\omega) = \cfrac{b_0^2}{\omega - a_0 - \cfrac{b_1^2}{\omega - a_1 - \cfrac{b_2^2}{\omega - a_2 - \cfrac{b_3^2}{\omega - a_3 - \cdots}}}}. \tag{4}$$

The recursion coefficients a_i and b_i are computed from the tridiagonalization of the tight-binding Hamiltonian matrix for a given starting orbital. The multiband terminator [17] is chosen to close the continued fraction. We have computed all assumed ordered states and the CE-AFM state observed experimentally in an enlarged supercell (16 primitive cells) and computed 27 levels for each of the 272 independent orbitals. Our results have been checked for different levels to ensure an energy accuracy better than 5 meV. The whole procedure is iterated self-consistently until convergence is reached and the density of states is obtained from $\rho_{ms}(\omega) = -\frac{1}{\pi} \operatorname{Im} G_{ms}(\omega)$, which allows us to compute the electron numbers and magnetic moments as well as the total energies of all the ordered states.

3. Numerical results and discussions

The band-structure parameters of $La_{1/2}Sr_{3/2}MnO_4$ used in our numerical calculation come from their counterpart, the cubic perovskite $LaMnO_3$, because the sizes of the Mn–O_6 octahedra of the two compounds are essentially the same; they are obtained by fitting the cluster-model photoemission spectra of the valence band [18]. As the Slater–Koster parameters approximately satisfy the scaling relation, they are taken as $(pd\sigma) = -2.0$ eV, $(pd\pi) = 0.922$ eV, $(pp\sigma) = 0.6$ eV, and $(pp\pi) = -0.15$ eV. The nearest-neighbour hopping integrals for the oxygens of neighbouring layers can be obtained using the formula [19] $V_{ll'm} = \eta_{ll'm}(\hbar^2/md^2)$ with d denoting the interatomic distance. The on-site Coulomb repulsion and Hund coupling constant are set as $U = 5.0$ eV and $j = 0.80$ eV. The bare on-site energy of the O p orbital is taken as the energy reference point $\varepsilon_p = 0$ eV; the bare on-site energy of Mn d depends on the Coulomb repulsion, $\varepsilon_d^0 = -13$ eV. The strength of the crystal-field splitting is set as $Dq = 0.10$ eV. The lattice parameters of $La_{1/2}Sr_{3/2}MnO_4$ with tetragonal symmetry are taken $a = b = 3.86$ Å and $c = 12.44$ Å from [7]. When JTD is taken into account, the nearest-neighbour O–O hopping integrals are modified by the above scaling relation while the integrals for hopping between Mn d and O p are given by another formula: $V_{ll'm} = \eta_{ll'm}(\hbar^2/md^{3.5})$ [19].

Since e_g electrons of Mn ions have strong itineracy in $La_{1/2}Sr_{3/2}MnO_4$ due to strong double-exchange interaction, the first ordered state to be considered is the FM state with uniform $d_{x^2-y^2}$ OO. Since the strong superexchange interaction between half-filled t_{2g} orbitals favours AFM coupling and can be accompanied by a certain amount of CO [20], the G-AFM state with the same $d_{x^2-y^2}$ OO is also chosen as a candidate for comparison with *charge ordering* in the CE-AFM state. In order to clarify the origin of the CE-AFM state as well as its corresponding $d_{3x^2-r^2}/d_{3y^2-r^2}$ OO, two other OO states in the CE-AFM state, i.e., uniform $d_{x^2-y^2}$ and $d_{3z^2-r^2}$ OO states, are also investigated. The HF calculation is carried out self-consistently and all ordered states above are taken as initial trial states. As both experimental observation and band-structure calculation confirm that Mn^{3+}-like sites have a considerable JTD, we take in our calculation the most favourable JTD mode on those OO states while keeping the whole crystal volume constant; e.g., the $d_{x^2-y^2}$ orbital favours JTD mode $(Q, Q, -2Q)$ and $d_{3x^2-r^2}$ corresponds to the $(2Q, -Q, -Q)$ mode, with Q $(Q > 0)$ denoting the lattice distortion variable. We neglect the tilting of MnO_6 octahedra and the breathing mode (Q, Q, Q) (the volume of the Mn^{3+}-like site bulges and that of the Mn^{4+}-like site contracts), because recent first-principles band calculations [11] and x-ray scattering experiments [21] did not detect this distortion mode. Our numerical results suggest that there is no CO evident in real space, so the first term in equation (3) does not contribute to the total energy of the system.

We perform the unrestricted HF calculation on these ordered states in the presence of JTD; the energies of various states are presented in figure 2. Without JTD, the FM state with uniform $d_{x^2-y^2}$ OO is the lowest in energy and the CE-AFM state with $d_{3x^2-r^2}/d_{3y^2-r^2}$ OO (L_1) is the second lowest, while the G-AFM state is the highest. This indicates that e_g electrons in $La_{1/2}Sr_{3/2}MnO_4$ have very strong itineracy, so the system tends to exhibit FM. However, when JTD increases, the energy difference between FM and CE-AFM decreases and L_1 'outdoes' the FM state at $d_L/d_A = 1.06$ (d_L denotes the longer Mn–O bond length within JTD and d_A is the average Mn–O bond length without JTD). This case is similar to that in $LaMnO_3$. As is well known, the ground state of $LaMnO_3$ is the A-type AFM insulator where spins of Mn ions are parallel in the MnO_2 plane (ab-plane) and antiparallel along the c-direction; this state is also accompanied by a considerable lattice distortion and the $d_{3x^2-r^2}/d_{3y^2-r^2}$ OO occurs throughout the whole crystal. Much study [22, 23] has shown that this magnetic structure in $LaMnO_3$ results from the competition between the AFM superexchange interactions among t_{2g}

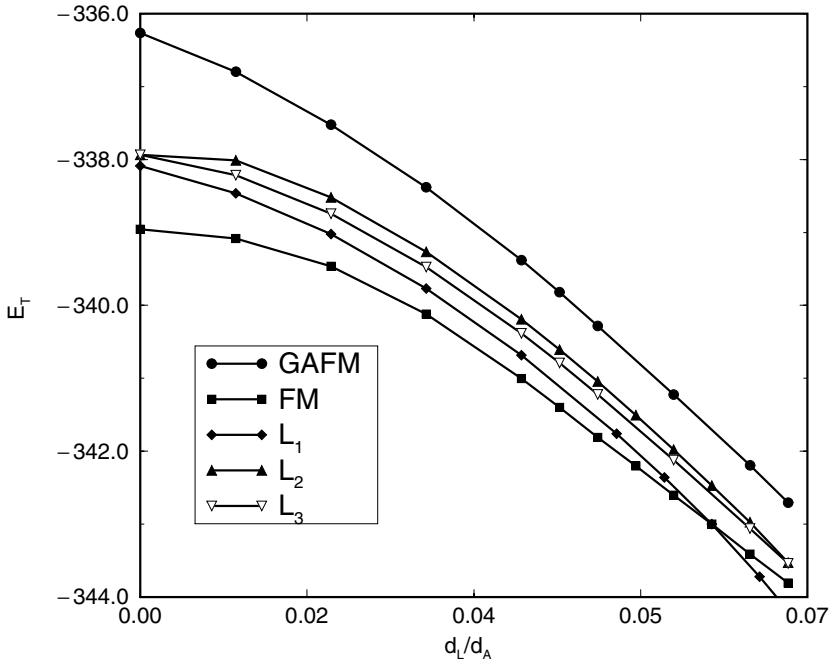

Figure 2. Energies per supercell unit (16 primitive cells) of the ordering states as functions of the JTD. They are the FM and G-AFM states with uniform $d_{x^2-y^2}$ OO, the CE-AFM state with $d_{3x^2-r^2}/d_{3y^2-r^2}$ OO (L_1), uniform $d_{x^2-y^2}$ (L_2), and $d_{3z^2-r^2}$ (L_3) OO.

electrons and the FM superexchange among e_g electrons. When the twofold degeneracy of the e_g orbital is lifted by JTD, the FM superexchange slightly decreases with the result that AFM order appears and the A-AFM state is one of the choices. In $La_{1/2}Sr_{3/2}MnO_4$, the CE-AFM state results from the competition between AFM superexchange among t_{2g} electrons and FM double exchange among e_g electrons. In the absence of JTD, the FM state with $d_{x^2-y^2}$ OO is the most stable state (see figure 2). From the purely ionic scenario, when JTD occurs, twofold-degenerate e_g orbitals of the Mn^{3+}-like site are split and only the lower energy level is occupied, while those of Mn^{4+}-like sites are not affected, since they are not Jahn–Teller-active ions. JTD reduces the e_g bandwidth and AFM spin ordering may appear in the compound.

The FM zigzag chains couple antiferromagnetically with each other in the CE-AFM state and this can be understood from its diagonal $d_{3x^2-r^2}/d_{3y^2-r^2}$ OO. In $LaMnO_3$ with the A-type AFM ground state, the FM superexchange between the neighbouring $d_{3x^2-r^2}$ ($d_{3y^2-r^2}$) and $d_{x^2-z^2}$ ($d_{y^2-z^2}$) orbitals along the *a*-direction (*b*-direction) in the *ab*-plane is double that along the *c*-direction, so, as discussed above, the magnetic coupling along the *c*-direction is antiferromagnetic when lattice distortion occurs. Here, $La_{1/2}Sr_{3/2}MnO_4$ similarly undergoes $d_{3x^2-r^2}/d_{3y^2-r^2}$ OO of Mn^{3+}-like sites, thus gaining the maximized kinetic energy (compare L_1 with L_2 and L_3, as shown in figure 2). The intensity of transfer of e_g electrons between $d_{3x^2-r^2}$ ($d_{3y^2-r^2}$) and $d_{x^2-y^2}$ along the direction of the orbital (we assume that $d_{3x^2-r^2}$ ($d_{3y^2-r^2}$) has the x (y) orbital direction) is double that perpendicular to the orbital direction. Thus, when the JTD takes effect and the double-exchange interaction slightly decreases as discussed above, the FM ordering perpendicular to the orbital direction is replaced by AFM spin ordering while the FM coupling along the orbital direction is kept unchanged. It is the $d_{3x^2-r^2}/d_{3y^2-r^2}$ OO and JTD that lead to the CE-AFM magnetic structure as shown in figure 1.

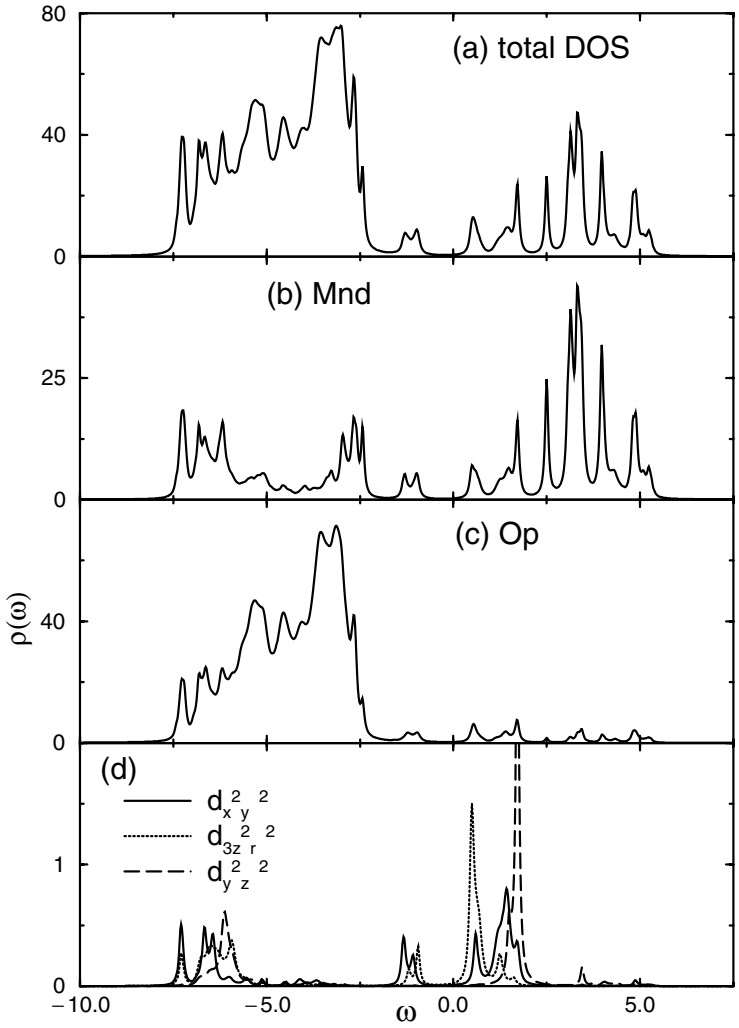

Figure 3. The density of states of the CE-AFM state with $d_{3x^2-r^2}/d_{3y^2-r^2}$ OO. (a) Total DOS, (b) PDOS of O p, (c) PDOS of Mn d, and (d) PDOS of the orbitals $d_{x^2-y^2}$, $d_{3z^2-r^2}$, and $d_{y^2-z^2}$ with the majority spin direction. The parameters are described in the text.

The total DOS of the CE-AFM state (L_1) is presented in figure 3(a); this state is an insulator since the Fermi energy ($E_F \equiv 0$) lies within the energy gap. The analysis of the partial DOS (PDOS) plotted in figures 3(b)–(d) reveals that the DOS below E_F is mainly contributed by O p orbitals. The peaks near the bottom and top of the valence band stem from Mn d orbitals due to the strong exchange splitting. The electron occupancies of the Mn^{3+}-like site and the Mn^{4+}-like site without JTD are almost the same, 4.62 and 4.61; their magnetic moments are the same: 3.63 μ_B. When JTD occurs, the difference in electron occupancy between them increases slightly (less than 0.1), because the energy level of the $d_{3x^2-r^2}$ or $d_{3y^2-r^2}$ orbital of the Mn^{3+}-like site is lowered slightly due to JTD—e.g., the occupancy of Mn^{3+} is 4.66 and that of Mn^{4+} is 4.59 at $d_L/d_A = 1.07$, while their magnetic moments are 3.72 and 3.50 μ_B. The overall spectrum profile is consistent with that resulting from a single-particle method. [13]

Inside the FM zigzag chain, the $d_{3x^2-r^2}$ or $d_{3y^2-r^2}$ orbital of the Mn^{3+}-like site can easily form a bonding state with the neighbouring $d_{x^2-y^2}$ orbital of a Mn^{4+}-like site. As is shown in figure 3(d), $d_{x^2-y^2}$ for Mn^{4+} ions lies partly below E_F, while the nonbonding state comes from the $d_{3z^2-r^2}$, $d_{y^2-z^2}$, and $d_{z^2-x^2}$ above E_F. Due to this strong effect of covalent bonding between the $d_{3x^2-r^2}$ ($d_{3y^2-r^2}$) and $d_{x^2-y^2}$ orbitals in the FM zigzag chain, the electron occupations of Mn^{3+} and Mn^{4+} ions do not differ greatly unless the difference between two single-energy levels is great. Since a pair of Mn^{3+} and Mn^{4+} ions possess only one e_g electron and this electron should occupy the bonding state, from band theory the system will be a band insulator, as shown in figure 3(a). It is the formation of the bonding state that, in the CE-AFM state (L_1), leads to there being no evident charge modulation in real space. The strong double-exchange interaction inside the FM chain makes it impossible for an electron to localize strongly at one site. This can also be seen for other mixed-valence systems (one ion has two different species with the ratio 1:1) with CO observed experimentally. For instance, in $YBaCo_2O_5$, the ratio of Co^{2+} and Co^{3+} ions is 1:1 and real-space charge ordering has been detected by synchrotron x-ray and neutron powder diffraction measurements [24, 25]. It was found that the occupations of Co^{2+} and Co^{3+} in the AFM ground state are respectively 7.18 and 6.64 [26], which indicates evident charge modulation from site to site. The difference between these two compounds is as regards the e_g electron interaction: there is an imaginary AFM superexchange process in $YBaCo_2O_5$, but a real double exchange in $La_{1/2}Sr_{3/2}MnO_4$. From the order of magnitude, the former is similar to second-order perturbation while the latter is a first-order perturbation. Hence, the *covalent bond* between Mn^{3+} and Mn^{4+} ions can easily form for strong double-exchange interaction and this would not result in an evident charge modulation in real space. In fact, the G-AFM state in our calculation in figure 2 is accompanied by an obvious CO. The electron occupancies of Mn^{3+} and Mn^{4+} ions are 3.45 and 3.72 for $d_L/d_A = 1.0$, respectively, and their magnetic moments are 3.87 and 3.24 μ_B, which suggests that the e_g electron should be much more difficult to localize in the FM state than in the AFM state.

4. Conclusions

In summary, we have shown, by using the HF approximation in the multiband d–p Hubbard model and the real-space recursion method, that the JTD and anisotropy of double exchange are the driving forces for the CE-AFM state in $La_{1/2}Sr_{3/2}MnO_4$ with $d_{3x^2-r^2}/d_{3y^2-r^2}$ OO. In our calculation, there is no evident charge modulation from site to site; this is attributed to the strong double-exchange interaction of e_g electrons inside the FM zigzag chain of the CE-AFM state.

Acknowledgments

The present work was supported in part by the National Natural Science Foundation of China under grant nos NSF 19677202, 10021001 and the 'Excellent Youth Foundation' [0025419] as well as the 'Climbing Programme' of the NSTC. We acknowledge with thanks CPU time on the SGI ORIGIN 2000 of the Laboratory of Computational Condensed Matter Physics.

References

[1] Kusters R M, Singleton J, Keen D A, McGreevy R and Hayes W 1989 *Physica* B **155** 362
Jin S, Teifel T H, McCormack M, Fastnacht R A, Ramesh R and Chen L H 1994 *Science* **264** 413
[2] See, e.g.,
Tokura Y and Nagaosa N 2000 *Science* **288** 462

[3] Kuwahara H *et al* 1995 *Science* **270** 961
Moritomo Y *et al* 1997 *Phys. Rev.* B **55** 7549
[4] Goodenough J B 1955 *Phys. Rev.* **100** 564
[5] Jirak Z, Krupicka S, Sima Z, Dlouha M and Vratislav S 1985 *J. Magn. Magn. Mater.* **53** 153
Radaelli P G, Cox D E, Marezio M, Cheong S-W, Schiffer P E and Ramirez A P 1995 *Phys. Rev. Lett.* **75** 4488
Radaelli P G, Cox D E, Marezio M and Cheong S-W 1997 *Phys. Rev.* B **55** 3015
Chen C H and Cheong S-W 1996 *Phys. Rev. Lett.* **76** 4042
[6] Sternlieb B J, Hill J P, Wildgruber U C, Luke G M, Nachumi B, Moritomo Y and Tokura Y 1996 *Phys. Rev. Lett.* **76** 2169
[7] Murakami Y, Kawada H, Kawata H, Tanaka M, Arima T, Moritomo Y and Tokura Y 1998 *Phys. Rev. Lett.* **80** 1932
[8] Solovyev I V and Terakura K 1999 *Phys. Rev. Lett.* **83** 2825
[9] Mizokawa T and Fujimori A 1997 *Phys. Rev.* B **56** R493
[10] Lee J, Yu J and Terakura K 1998 *J. Korean Phys. Soc.* **33** S55
[11] Mahadevan P, Terakura K and Sarma D D 2001 *Phys. Rev. Lett.* **87** 066404
[12] Anisimov V I *et al* 1997 *Phys. Rev.* B **55** 15 494
Koshibae W *et al* 1997 *J. Phys. Soc. Japan* **66** 957
[13] Jung J H, Ahn J S, Yu Jaejun, Noh T W, Lee Jinhyoung, Moritomo Y, Solovyev I and Terakura K 2000 *Phys. Rev.* B **61** 6902
[14] Mizokawa T and Fujimori A 1996 *Phys. Rev.* B **54** 5368
[15] Kugel K I and Khomskii D I 1982 *Sov. Phys.–Usp.* **25** 231
[16] Heine V, Haydock R and Kelly M J 1980 *Solid State Physics: Advances in Research and Applications* vol 35, ed H Ehrenreich, F Seitz and D Turnbull (New York: Academic) p 215
[17] Haydock R and Nex C M M 1984 *J. Phys. C: Solid State Phys.* **17** 4783
[18] Barman S R and Sarma D D 1994 *Phys. Rev.* B **49** 13 979
Abbate M, Fuggle J C, Fujimori A, Tjeng L H, Chen C T, Potze R, Sawatzky G A, Eisaki H and Uchide S 1993 *Phys. Rev.* B **47** 16 124
Zhuang M, Zhang W and Ming N 1997 *Phys. Rev.* B **56** 14 547
[19] Harrison W A 1980 *Electronic Structure and the Properties of Solids* (San Francisco, CA: Freeman)
[20] Tokunaga M, Miura N, Tomioka Y and Tokura Y 1998 *Phys. Rev.* B **57** 5259
Allodi G, De Renzi R, Licci F and Pieper M W 1998 *Phys. Rev. Lett.* **81** 4736
[21] Larochelle S, Mehta A, Kaneko N, Mang P K, Panchula A F, Zhou L, Arthur J and Greven M 2001 *Phys. Rev. Lett.* **87** 095502
[22] Sawada H, Moritomo Y, Terakura K and Hamada N 1997 *Phys. Rev.* B **56** 12 154
Maezono R, Ishihara S and Nagaosa N 1998 *Phys. Rev.* B **58** 11 583
[23] Solovyev I, Hamada N and Terakura K 1996 *Phys. Rev. Lett.* **76** 4825
Jackeli G, Perkins N B and Plakida N M 2000 *Phys. Rev.* B **62** 372
Ishihara S, Inoue J and Maekawa S 1997 *Phys. Rev.* B **55** 8280
[24] Vogt T, Woodward P M, Karen P, Hunter B A, Henning P and Moodenbaugh A R 2000 *Phys. Rev. Lett.* **84** 2969
[25] Suard E, Fauth F, Caignaert V, Mirebeau I and Baldinozzi G 2000 *Phys. Rev.* B **61** R11 871
[26] Wang J, Zhang Weiyi and Xing D Y 2001 *Phys. Rev.* B **64** 064418